INTERNATIONAL JOURNAL FOR NUMERICAL METHODS IN FLUIDS
Int. J. Numer. Meth. Fluids 2009; **60**:1241–1258
Published online 4 November 2008 in Wiley InterScience (www.interscience.wiley.com). DOI: 10.1002/fld.1946

Simulation of a turbulent channel flow with an entropic Lattice Boltzmann method

M. Spasov, D. Rempfer*, † and P. Mokhasi

Mechanical, Materials and Aerospace Engineering Department, Illinois Institute of Technology, 10 W 32nd St, Chicago, IL 60616, U.S.A.

SUMMARY

The Lattice Boltzmann method (LBM) is used to simulate turbulent channel flow. Two simulations are performed. One uses high enough grid resolution in order for it to be considered a direct numerical simulation (DNS). LBM in its traditional form is adopted for this simulation. The other simulation uses lower resolution for which the original method becomes unstable. An entropy condition is used to render this simulation stable. Results from these two numerical experiments are compared with the results from a DNS performed with traditional numerical techniques. It is concluded that LBM can be used as tool to simulate turbulent flows and entropy stabilized LBM schemes can be used to achieve accurate results with reasonably low grid resolution. Copyright © 2008 John Wiley & Sons, Ltd.

Received 19 May 2008; Revised 9 September 2008; Accepted 11 September 2008

KEY WORDS: LBM; Lattice; Boltzmann; entropy; channel flow; direct numerical simulation; numerical methods; incompressible flow; turbulence; Lattice Boltzmann method

1. INTRODUCTION

The Lattice Boltzmann method (LBM) [1, 2] is a novel numerical scheme for solving the equations governing fluid flows. Unlike traditional numerical techniques, LBM does not solve the macroscopic equations directly. It is based on the dynamics of fictional populations of particles the size of which is assumed to be at the mesoscopic scale (i.e. somewhere between the atomic scale and the macroscopic scale of the world we live in). These dynamics are described with a simple kinetic equation, which avoids solving the Boltzmann equation and obviates the need to follow each molecule, as in molecular dynamics simulations. The simplest form of the kinetic equation is the

*Correspondence to: D. Rempfer, Mechanical, Materials and Aerospace Engineering Department, Illinois Institute of Technology, 10 W 32nd St, Chicago, IL 60616, U.S.A.
†E-mail: rempfer@iit.edu

Contract/grant sponsor: ONR; contract/grant number: N000140510914

so-called Lattice Bhatnagar–Gross–Krook (LBGK) form

$$f_i(\mathbf{x}+\mathbf{c}_i, t+1) = f_i(\mathbf{x}, t) + \omega[f_i^{\mathrm{eq}}(\rho, \mathbf{u}) - f_i(\mathbf{x}, t)] \tag{1}$$

where the distribution function f_i is the only variable in this equation, $\mathbf{c}_i$ is the vector connecting a grid point with coordinates given by $\mathbf{x}$ to one of its immediate neighbors, ω is a relaxation parameter, which is directly related to the viscosity of the model, and f_i^{eq} is the equilibrium distribution function, which is dependent on the velocity $\mathbf{u}$ and density ρ at the grid point. All macroscopic variables emerge from the distribution function, and thus there is no need to solve a separate Poisson problem for the pressure, which otherwise often produces difficulties in numerical simulations and requires special attention. Following Keating *et al.* [3], one possible way to recover the Navier–Stokes equations from (1) is to take

$$f_i^{\mathrm{eq}}(\rho, \mathbf{u}) = W_i \rho[1 + 3c_{i\alpha}u_\alpha + \tfrac{3}{2}u_\alpha u_\beta(3c_{i\alpha}c_{i\beta} - \delta_{\alpha\beta})] \tag{2}$$

$$\nu = \frac{1}{6}\left(\frac{2}{\omega} - 1\right), \quad \rho = \sum_i f_i \tag{3}$$

$$p = \frac{\rho}{3}, \quad u_\alpha = \sum_i f_i c_{i\alpha} \tag{4}$$

with implied summation over the spatial indices denoted by Greek letters. For three-dimensional simulations the computationally least cumbersome approach results from the so-called D_3Q_{15} model. It was used for all the simulations in the current study. This model requires 15 directions of the distribution function at each grid point and it was shown recently [4] that little, if any, increase in accuracy is achieved through adding more directions. The 15 directions of the distribution function at each grid point are updated according to the following algorithm:

1. *Collision*—The local density and subsequently the flow velocity are computed from (2) and (3) based on the current configuration. The summation is over all 15 directions. Then the local equilibrium function is computed based on Equation (4). A new set of populations are taken as

$$f_i'(\mathbf{x}, t) = f_i(\mathbf{x}, t) + \omega[f_i^{\mathrm{eq}}(\rho, \mathbf{u}) - f_i(\mathbf{x}, t)] \tag{5}$$

2. *Streaming*—The new populations are moved to their corresponding neighbor:

$$f_i(\mathbf{x}+\mathbf{c}_i, t) = f_i'(\mathbf{x}, t) \tag{6}$$

The kinetic equation (1) provides some features that are missing in the traditional macroscopic solvers: intuitive representation of the microscopic dynamics governing the macroscopic behavior, locality of particle interactions, which leads to perfectly parallel computational algorithms, and simplicity when it comes to including additional physics in the simulation such as magnetic fields, multiphase flows, etc.

Now we turn our attention to numerical stability. Historically, the LBM originated from cellular automata [5, 6], and it possesses all the properties associated with them. One of these characteristics—nonlinear stability through obeying a H-theorem—had to be abandoned in order to make the method competitive with the rest of the numerical techniques used in computational fluid dynamics. Without it, however, LBM became susceptible to a wide variety of numerical instabilities, which are not well understood and are considered to be among the main obstacles

DOI: 10.1002/fld

to a wider application of the technique [4, 7]. This problem was experienced in the current study also. A possible fix is to modify the model (essentially, by adjusting the effective viscosity) so that its dynamics obey a H-theorem. The new method is termed *entropic Lattice Boltzmann method* or ELBM for short. The quantity H in statistical physics is defined as

$$H = \int \phi \log \phi \, \mathrm{d}\mathbf{c} \, \mathrm{d}\mathbf{r} \tag{7}$$

where $\phi(\mathbf{r}, \mathbf{c}, t)$ is the distribution function such that $\phi \, \mathrm{d}\mathbf{r} \, \mathrm{d}\mathbf{c}$ is the number of molecules at time t positioned between $\mathbf{r}$ and $\mathbf{r}+\mathbf{d}r$, which have velocities in the range $\mathbf{c}$ to $\mathbf{c}+\mathbf{d}c$ (cf. the LBM distribution function f). The H-theorem states that

$$\partial_t H \leqslant 0 \tag{8}$$

which is why the entropy, in its statistical physics definition

$$S = -k_\mathrm{B} H \tag{9}$$

(k_B is the Boltzmann constant) is non-decreasing with time

$$\partial_t S \geqslant 0 \tag{10}$$

The move from cellular automata to the LBGK equation (1) had completely abandoned the concept of a H-theorem.

The issue is not yet solved and is a topic of ongoing research [4, 7]. One approach that has been proposed [7] is to take an LBM-suitable discretization of (7):

$$H(\mathbf{f}) = \sum_i f_i \ln\left(\frac{f_i}{W_i}\right) \tag{11}$$

with W_i the same as in (4). Next, change the form of the governing equation to

$$f_i(\mathbf{x}+\mathbf{c}_i, t+1) = f_i(\mathbf{x}, t) + \alpha\beta[f_i^{\mathrm{eq}}(\mathbf{x}, t) - f_i(\mathbf{x}, t)] \tag{12}$$

where α is the solution of

$$H(\mathbf{f}') = H(\mathbf{f}) \tag{13}$$

with $\mathbf{f}'$ and $\mathbf{f}$ denoting the post-collision and pre-collision states, respectively (cf. Equation (5)). The needed amount of dissipation is brought in through the coefficient

$$\beta = \frac{1}{6\nu+1} \tag{14}$$

The regular LBGK is recovered if $\alpha = 2$. In simulations, the solution to (13) is very close to this value within most of the domain.

The goal of the current study is to apply LBM to turbulent flows so that they can be simulated within a more efficient and flexible framework. Although much research has been done on the lattice Boltzmann method, its particular application to turbulent flows has barely been investigated [8]. Since the ability of today's computers prohibits the use of all the grid points needed, turbulence models or large eddy simulations are often employed. In order to develop these for LBM one must make sure that it is capable of direct numerical simulations (DNS) of turbulence first. Following

DOI: 10.1002/fld

this logic, the fully developed incompressible, pressure-driven turbulence between two parallel plates was chosen as a test problem for DNS. Next, ELBM was employed for the same problem with a significantly decreased grid resolution and the results are compared and discussed.

2. PROBLEM STATEMENT

2.1. Description in terms of macroscopic variables

Flow between two parallel flat plates of infinite length with periodic boundary conditions in the two spatial directions, which are parallel to these walls is referred to as channel flow (Figure 1). It is driven either by a constant pressure gradient (body force) or a constant mass flux. At a high enough Reynolds number this flow is turbulent and is often used to study fundamental properties of wall-bounded turbulent flows.

The domain is considered infinite in the streamwise and spanwise directions (x and z, respectively). A no-slip condition is enforced in the wall-normal direction at the flat plates, which are at $y=0$ and $y=2H$. Fully developed turbulence is observed at high enough Reynolds numbers when the flow has reached a statistically steady state. The transition to turbulence is not of interest in this study.

The macroscopic quantities of interest are pressure and velocity. To make the comparison of our results with the already existing data easier, let us first examine how the problem is analyzed theoretically. The instantaneous flow field is decomposed into a mean and a fluctuating component:

$$\tilde{u}_\alpha = U_\alpha + u_\alpha \tag{15}$$

$$\tilde{p} = P + p \tag{16}$$

Substituting these in the Navier–Stokes equations one can obtain the Reynolds momentum equation for the mean flow:

$$U_\beta \frac{\partial U_\alpha}{\partial x_\beta} = \frac{1}{\rho}\frac{\partial}{\partial x_\beta}(-P\delta_{\alpha\beta} + 2\mu S_{\alpha\beta} - \overline{\rho u_\alpha u_\beta}) \tag{17}$$

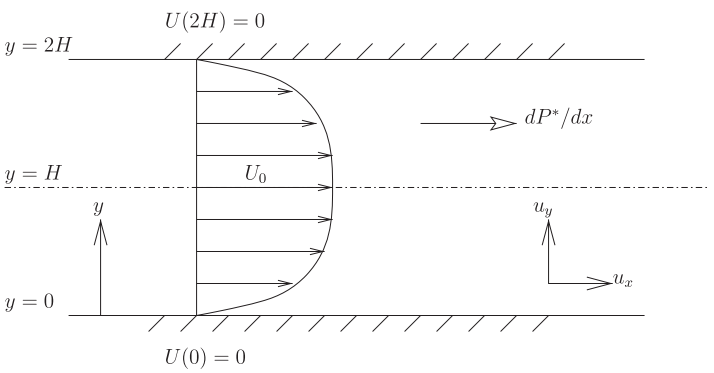

Figure 1. Schematic of a channel flow. The third dimension is not shown for simplicity.

DOI: 10.1002/fld

where $\tau_{\alpha\beta}=\overline{\rho u_\alpha u_\beta}$ represents the correlation between the velocity fluctuations in different directions and is called the Reynolds stress tensor. The theoretical analysis for the channel flow described above continues by assuming that the mean flow is steady, has an x-velocity component only, and all derivatives of mean quantities, normal to the x–y-plane are zero. All derivatives in the x-direction are also assumed to vanish except for the pressure gradient $\mathrm{d}P/\mathrm{d}x$. The analysis is restricted to the bottom half channel where $y=(0, H)$. The results are also valid for the upper half because of symmetry. The remaining terms in the x- and y-momentum equations are

$$0=-\frac{1}{\rho}\frac{\partial P}{\partial x}-\frac{\mathrm{d}}{\mathrm{d}y}\overline{uv}+\nu\frac{\partial^2 U}{\mathrm{d}y^2} \tag{18}$$

$$0=-\frac{1}{\rho}\frac{\partial P}{\partial y}-\frac{\mathrm{d}}{\mathrm{d}y}\overline{v^2} \tag{19}$$

Integration of (19) gives

$$\frac{P(y)-P(y=0)}{\rho}+\overline{v^2}(y=0)=\frac{P-P^*}{\rho}+\overline{v^2}=0 \tag{20}$$

and subsequent differentiation in x leads to equality of $\partial P/\partial x$ and $\mathrm{d}P^*/\mathrm{d}x$. Therefore, (18) can be integrated from $y^*=0$ to y to get

$$0=-\frac{1}{\rho}\frac{\partial P^*}{\partial x}y-\overline{uv}+\nu\frac{\mathrm{d}U}{\mathrm{d}y}-u_\tau^2 \tag{21}$$

where the friction velocity is defined as

$$u_\tau^2=\nu\frac{\mathrm{d}U}{\mathrm{d}y}\bigg|_{y=0} \tag{22}$$

At the center of the channel ($y=H$) the shear stress has to be zero in order for the velocity profile to be symmetric:

$$-\overline{uv}+\nu\frac{\mathrm{d}U}{\mathrm{d}y}=0 \tag{23}$$

This means that the friction velocity can be found if the pressure gradient and channel height are given:

$$u_\tau^2=-\frac{\mathrm{d}P^*}{\mathrm{d}x}\frac{H}{\rho}=-\frac{\mathrm{d}P}{\mathrm{d}x}\frac{H}{\rho} \tag{24}$$

Using this to substitute the pressure gradient in (21), one obtains

$$-\overline{uv}+\nu\frac{\mathrm{d}U}{\mathrm{d}y}=u_\tau^2\left(1-\frac{y}{H}\right) \tag{25}$$

which has to be solved in order to get the profile of the mean velocity. To proceed analytically, the channel is divided into a core region and a surface layer in the wall-normal direction with a

DOI: 10.1002/fld

common inertial sublayer between them [9]. The solution for the velocity profile in the inertial sublayer is given by

$$\frac{U}{u_\tau} = \frac{1}{\kappa} \ln y_+ + a \tag{26}$$

where $y_+ = y u_\tau / \nu$ is the non-dimensionalized y-coordinate, $\kappa \approx 0.4$ is the von Karman constant, and $a \approx 5.2$ can be found from experimental data. By comparing the velocity profiles in the core region and the surface layer, it follows that [9]

$$\frac{U_0}{u_\tau} = \frac{1}{\kappa} \ln Re_\tau + b \tag{27}$$

where $b \approx 6$ is again obtained from experimental data and $Re_\tau = u_\tau H / \nu$. This is the so-called logarithmic friction law, which determines the mean velocity at the center of the channel U_0 from the pressure gradient and the channel height (used with (24)).

2.2. *DNS with LBM—simulation setup*

Turbulent channel flow simulations with LBM have been done by other researchers in the past [8, 10]. The main interest in the current study is whether the LBM and its entropic modification are going to be able to accurately reproduce the mean velocity and pressure profiles, the Reynolds stress components, and the r.m.s. pressure fluctuations. In order to obtain converged statistical quantities the simulation has to be carried out in several steps. First, the initial state is taken as a superposition of the analytic solution for the mean velocity profile and fluctuations taken from a spectral DNS simulation and interpolated for use on the current grid. Second, the simulation has to be run long enough so that mean fields are converged. Finally, once these are available, the required statistics of the fluctuating fields can be accumulated.

Except for the Reynolds number of the simulation, one has to also decide how big the domain will be. For this purpose, the aspect ratios $\alpha_x = L_x / H$ and $\alpha_z = L_z / H$ are defined. The authors of [11] did a study on what the size of the computational domain should be so that it could maintain a turbulent flow field and give good results for different Reynolds numbers (referred to as a minimal channel flow). Based on their study the computational domain here was taken with $\alpha_x = 4$ and $\alpha_z = 1$.

The no-slip condition at the flat plates is enforced by using the halfway bounce-back scheme (see, for example, [12]). This choice was made because other schemes either introduced instabilities or did not give good accuracy near the boundary, which introduces an error into the results throughout the domain. The driving pressure gradient was replaced by an equivalent body force [13]. Periodicity was implemented for the distribution functions in both the spanwise and streamwise directions.

Once Re_τ for the simulation is chosen, the value of u_τ and the grid size are selected based on numerical resolution requirements. For a DNS the grid size Δ should not exceed the local Kolmogorov length scale η. Usually, the smallest scales for channel flow turbulence are near the wall, which is why often most of the grid points are concentrated there. For the LBM with a uniform grid, this strategy is unfortunately not possible and the grid resolution has to be the same everywhere. This disadvantage is partially compensated by the LBM's easy amenability to parallel

DOI: 10.1002/fld

coding. A value for $\eta_0 = \eta(y \to 0)$ is needed to compute the size of the smallest grid element. With this in mind, consider

$$\eta_0^+ = \eta_0 \frac{u_\tau}{\nu} = \left(\frac{\nu^3}{\varepsilon}\right)^{1/4} \frac{u_\tau}{\nu} = \left(\varepsilon_0 \frac{\nu}{u_\tau^4}\right)^{-1/4} = (\varepsilon_0^+)^{-1/4} \tag{28}$$

where the standard definitions for the Kolmogorov microscales have been used. From the DNS data of Kim *et al.* [14], the dissipation has a maximum at the wall and when normalized by the viscous scales this maximum is given by $\varepsilon_0^+ \approx 0.2$. This corresponds to $\eta_0^+ = 1.5$. Since in LBM $\Delta = 1$,

$$\eta_0^+ = 1.5 \geqslant \Delta_+ = \Delta \frac{u_\tau}{\nu} = \frac{u_\tau}{\nu} \;\Rightarrow\; \frac{u_\tau}{\nu} \leqslant 1.5 \tag{29}$$

For $Re_\tau = u_\tau H/\nu = 180$ the channel half height has to be $H \geqslant 120$ if the simulation is to be considered a DNS.

Next, the kinematic viscosity and pressure gradient have to be prescribed. One additional constraint in LBM is that the maximum velocity has to be smaller than 0.1. The maximum of the mean velocity is at the center of the channel and can be substituted into the logarithmic friction law (27) to get an estimate for the friction velocity

$$u_\tau = \frac{U_0}{2.5 \ln Re_\tau + 6} \tag{30}$$

From here, the viscosity and pressure gradient are

$$\nu = \frac{u_\tau H}{\rho} \tag{31}$$

$$G = \frac{u_\tau^2 \rho}{H} \tag{32}$$

and ρ is initialized to a given constant value in the beginning of the simulation.

In the current study, the initialization was done from the data of a pseudo-spectral DNS. The grid resolution used is $513 \times 257 \times 129$ in the streamwise, wall-normal, and spanwise directions, respectively. Together with the viscosity and body force, which were prescribed, it corresponds to $Re_\tau = 179$. The code for the simulation was parallelized with MPICH2, and 36 processors were used. The computation time for one lattice time step was 4.5 s and the flow was evolved over approximately 1.2×10^6 time steps. The averaged statistics were computed based on the last 4.3×10^5 time steps for which the velocity and pressure field were saved every 500 time steps. The choice was made because it took the flow very long to reach a steady turbulent state. Performance comparison between DNS with LBM and DNS with pseudo-spectral methods was done by Lammers *et al.* [8]. They concluded that LBM is more efficient than pseudo-spectral methods and it would remain more efficient in the future when DNS of channel flow for higher Reynolds numbers will be possible.

2.3. Results from the DNS

Figures 2 and 3 give a general view of the instantaneous flow structures. The vorticity magnitude is largest near the wall and periodicity is enforced in the spanwise (z) and streamwise (x) directions.

DOI: 10.1002/fld

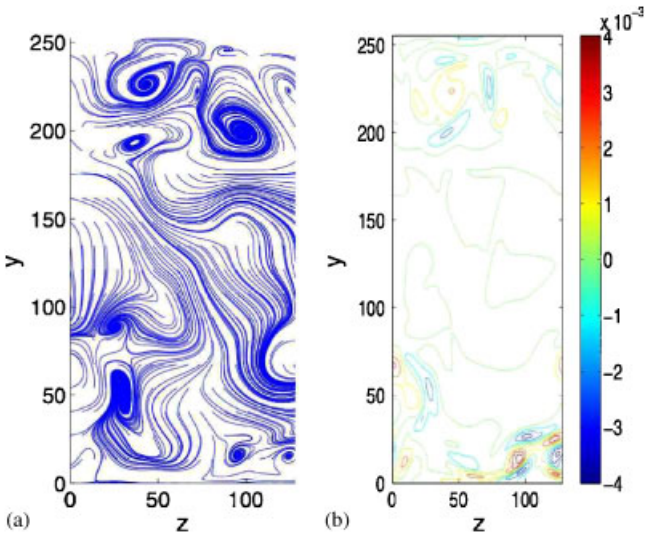

Figure 2. Instantaneous flow pattern for a cross section of the channel: (a) velocity pattern at a constant streamwise location and (b) vorticity at a constant streamwise location.

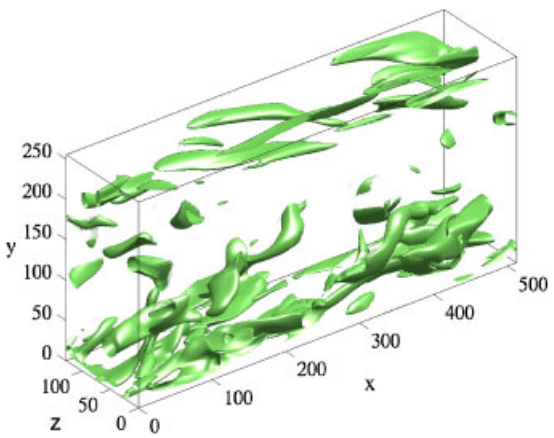

Figure 3. Snapshot of isosurfaces of the streamwise vorticity. Flow is from left to right in the x-direction. The two parallel plates are $y=0$ and $y=255$.

Figure 4 shows that the velocity profiles are not exactly the same at the two walls, which means that the flow needs more time to produce a symmetric profile and consequently a statistically converged one (note that statistical convergence is different from just convergence). This is also verified if one examines the mean velocity profiles averaged only over the last 107 500 time steps (Figure 5). Even with a smaller averaging time interval the profiles are closer to their desired shape. Considering the rate of change of the profiles, however, much more computational time

DOI: 10.1002/fld

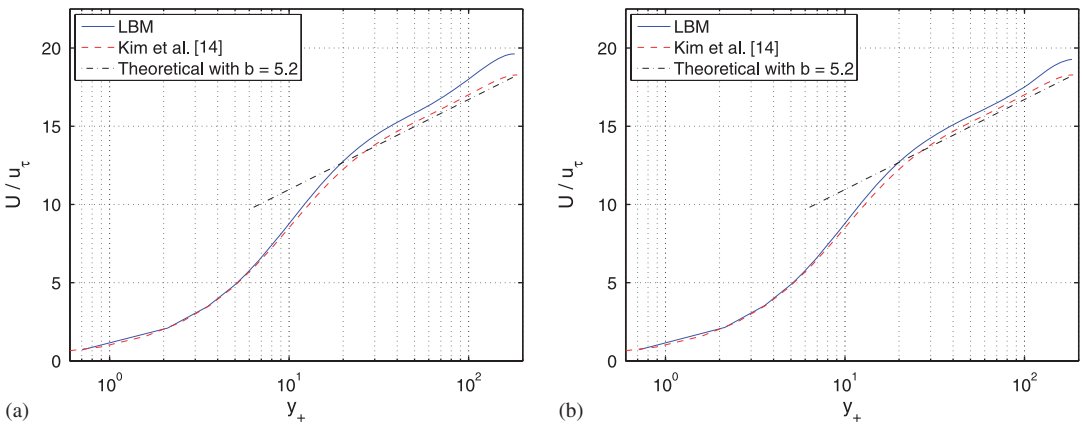

Figure 4. Comparison of LBM and traditional pseudo-spectral methods for mean velocity profiles. Averages are taken in time and space over 4.3×10^5 time steps. Based on the input parameters the theoretical value of Re_τ is 179: (a) upper wall ($Re_\tau = 179$) and (b) lower wall ($Re_\tau = 182$).

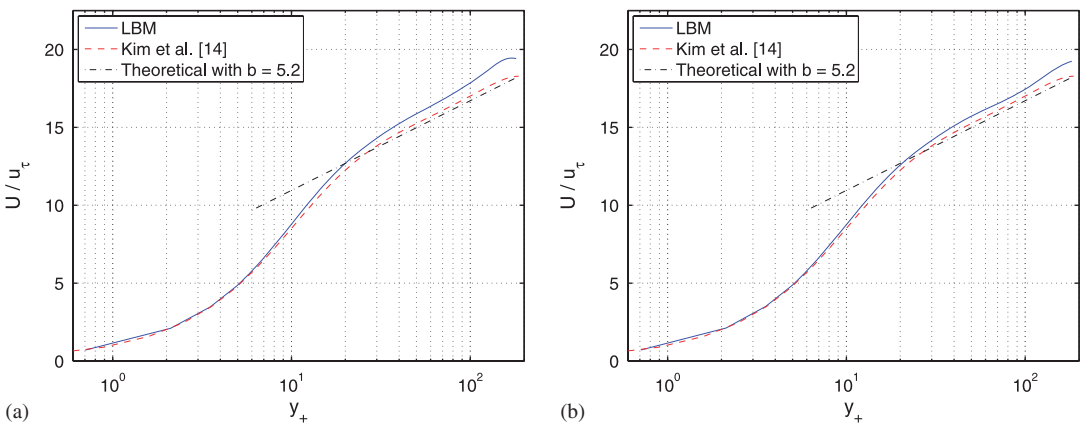

Figure 5. Comparison of LBM and traditional pseudo-spectral methods for mean velocity profiles. Averages are taken in time and space over the last 107.5 thousand time steps: (a) upper wall ($Re_\tau = 179$) and (b) lower wall ($Re_\tau = 181$).

would have been needed in order for them to match perfectly and that is why a longer run was not pursued.

Overall, LBM predicts slightly higher mean velocities but their time evolution shows slow decrease, which would probably lead to a much better fit at the end. The figures also show the computed Re_τ based on the simulation results. The value given by theory, based on the input parameters for the simulation, is 179. The results from the last 107 500 time steps give a more accurate Reynolds number at the lower wall. Again, this is an indication that the flow has not quite reached the steady statistical state. The mean wall-normal and especially spanwise velocities

DOI: 10.1002/fld

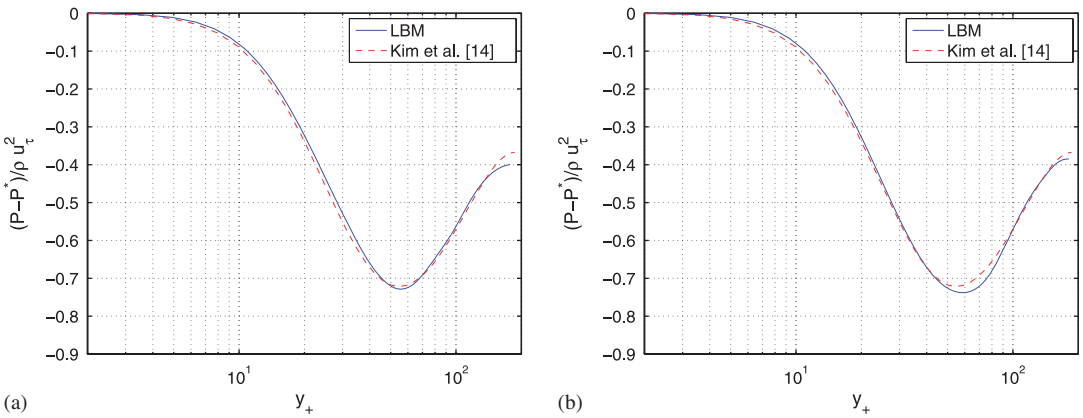

Figure 6. Comparison of LBM and traditional pseudo-spectral methods for mean pressure profiles. Averages are taken in time and space over 4.3×10^5 time steps: (a) upper wall ($Re_\tau = 179$) and (b) lower wall ($Re_\tau = 182$).

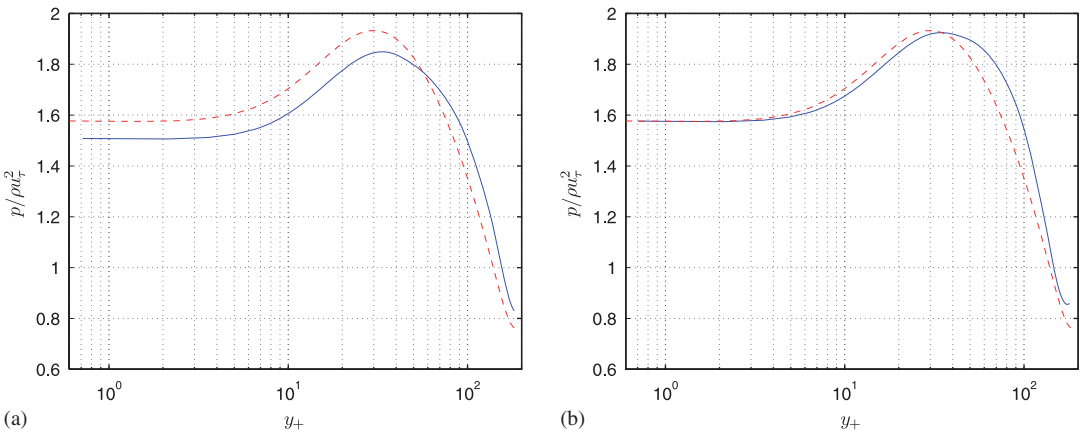

Figure 7. Comparison of LBM and traditional pseudo-spectral methods for the r.m.s. values of the pressure fluctuations at the lower and upper walls. Averages are taken in time and space over 4.3×10^5 time steps. Line styles as in Figure 4: (a) lower wall and (b) upper wall.

(Figure 9) are not zero. Their magnitude decreases but very slowly in time. The spanwise velocity is much greater than the wall-normal one, which might be due to the periodicity in this direction and the fact that the channel is the smallest in z.

Pressure in LBM is proportionally related to the change in density. Considering that the results are compared with the results from the DNS of incompressible turbulent flow, their good agreement is not expected. The pressure is non-dimensionalized following Equation (20). Figure 6 shows that the mean pressure profiles are very close to the ones given by the pseudo-spectral DNS. Pressure fluctuation profiles (Figure 7) seem to be in less of an agreement especially at the lower wall. The results also confirm the analytical relation between mean pressure and the wall-normal velocity

DOI: 10.1002/fld

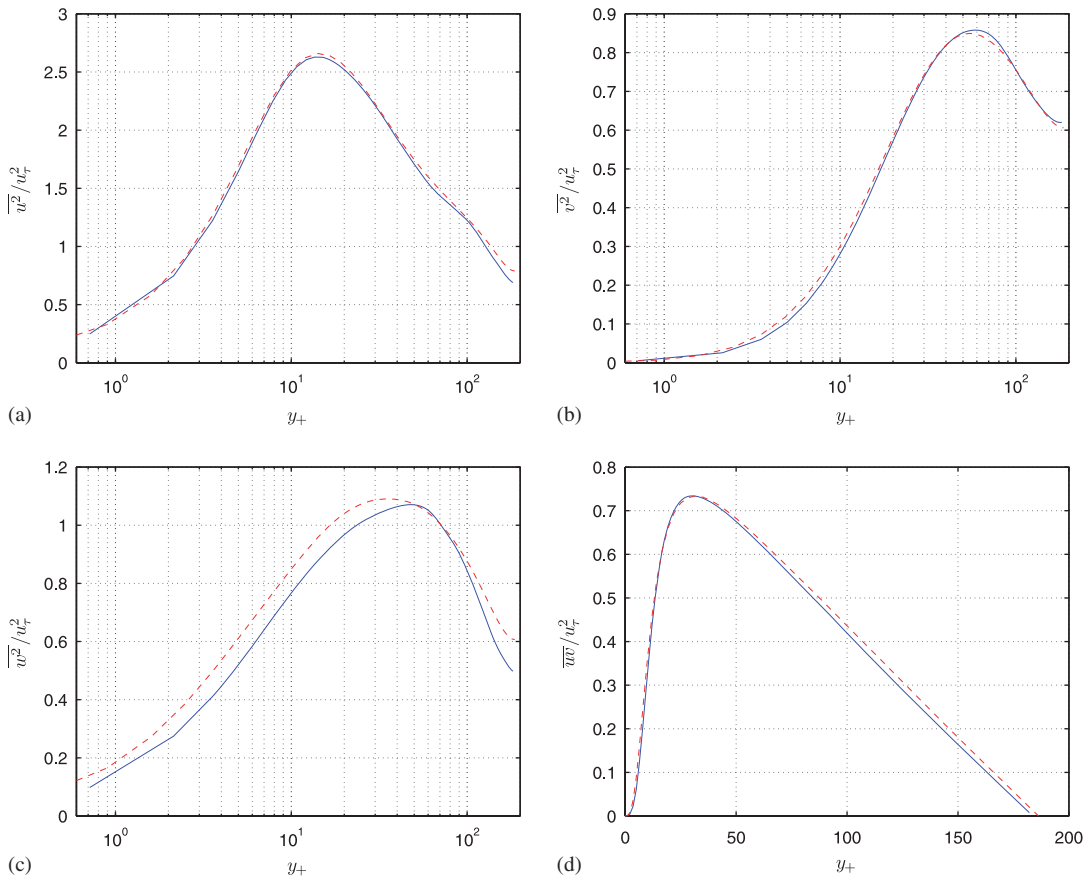

Figure 8. Comparison of LBM and traditional pseudo-spectral methods for Reynolds stresses at the lower wall. Averages are taken in time and space over 4.3×10^5 time steps. Line styles as in Figure 4.

fluctuations—as seen in Figure 10. It can be seen in the same figure how the mean pressure is distributed with the halfway bounce-back scheme. In the current study P^*, as shown, was chosen to non-dimensionalize the pressure.

Reynolds stresses are in very good agreement with the results from pseudo-spectral DNS (Figure 8). At both walls the profiles look the same and only the ones at the lower wall are shown here. There is a slight discrepancy for the spanwise velocity fluctuations. Again, this could be because the spanwise length of the channel is the smallest when compared with the others and because of the periodicity enforced in this direction.

Figure 11 shows the two-point spatial autocorrelation function

$$R_{ij}(\mathbf{r}, t) = \langle u_i(\mathbf{x}+\mathbf{r}, t) u_j(\mathbf{x}, t) \rangle \tag{33}$$

for the velocity fields at two different wall-normal heights (angle brackets denote suitable time average). Normalization is with respect to the first point, which makes the value there a maximum equal to one. The most noticeable feature is that there is no clear decay to zero even at the center

DOI: 10.1002/fld

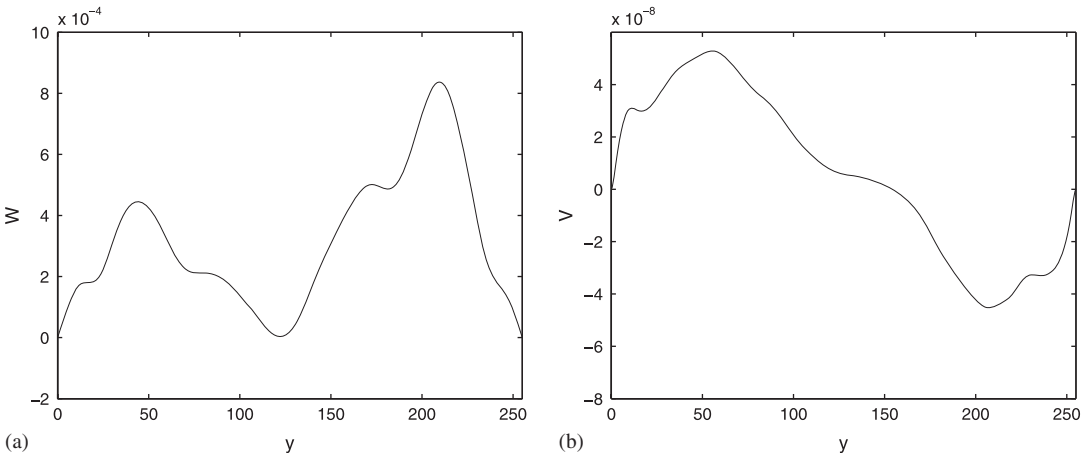

Figure 9. Convergence to statistically steady turbulent channel code: (a) spanwise mean velocity and (b) wall-normal mean velocity.

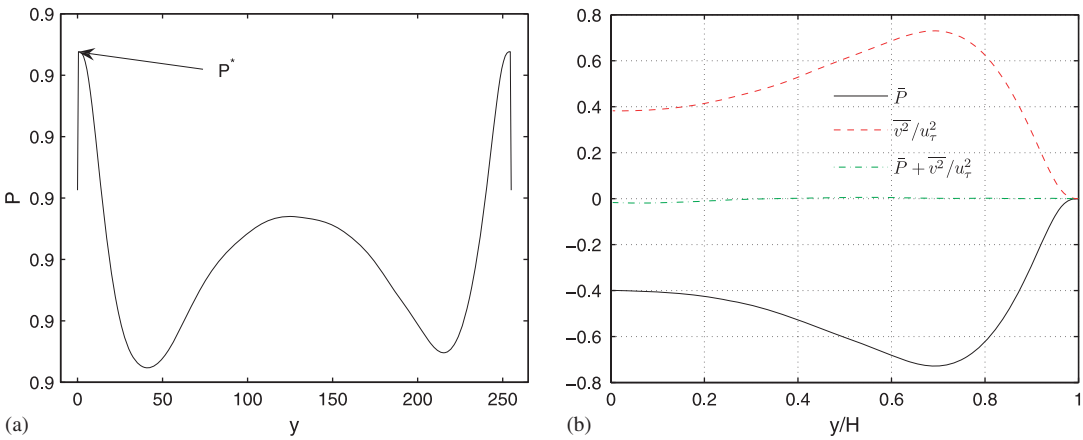

Figure 10. Mean pressure profiles with LBM. Averages are taken in time and space over 4.3×10^5 time steps: (a) mean pressure profile in lattice units. P^* is chosen at the first grid point next to the wall and (b) confirmation of the analytical relation between the mean pressure and the wall-normal velocity fluctuations.

of the channel. This means that the computational domain is not long enough for the most distant points to be uncorrelated. This is a consequence of the domain representing a minimal channel as described by Jimenez and Moin [11].

Figure 12 shows the one-dimensional spectra. By definition they are given as the Fourier transform of the two-point spatial correlation:

$$F_{ij}(k_1)=2\frac{1}{2\pi}\int_{-\infty}^{+\infty}R_{ij}(r_1,0,0)\exp(-\mathrm{i}k_1r_1)\,\mathrm{d}r_1 \tag{34}$$

DOI: 10.1002/fld

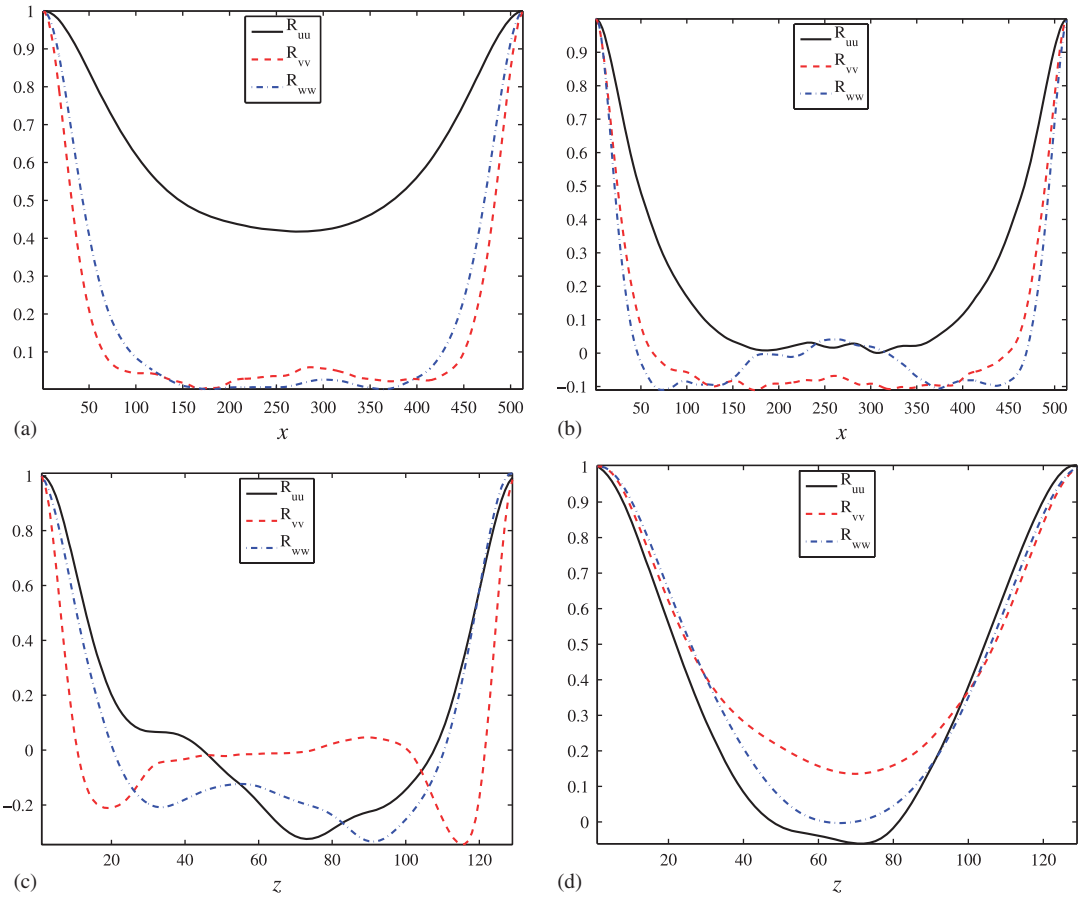

Figure 11. Two-point correlations: (a) $y_+ = 5.39$ (streamwise separation); (b) $y_+ = 149.23$ (streamwise separation); (c) $y_+ = 5.39$ (spanwise separation); and (d) $y_+ = 149.23$ (spanwise separation).

The wave number and the spectra themselves are non-dimensionalized with the friction velocity and channel half height:

$$F_{ij} = \frac{|F_{ij}|}{u_\tau^2 H}, \quad k = kH \tag{35}$$

When computing the discrete Fourier transform the correlation function for the whole length of the domain is considered.

2.4. *ELBM and results from it*

In order to apply ELBM on a grid with a smaller number of points, one has to first scale the results from the LBM DNS so that they can be used as an initial condition of the new simulation. Above, the non-dimensional dissipation was used to determine the necessary number of grid points. Here, this is not a requirement. Instead, the gradient at the wall $\mathrm{d}U/\mathrm{d}y$ is computed from the interpolated

DOI: 10.1002/fld

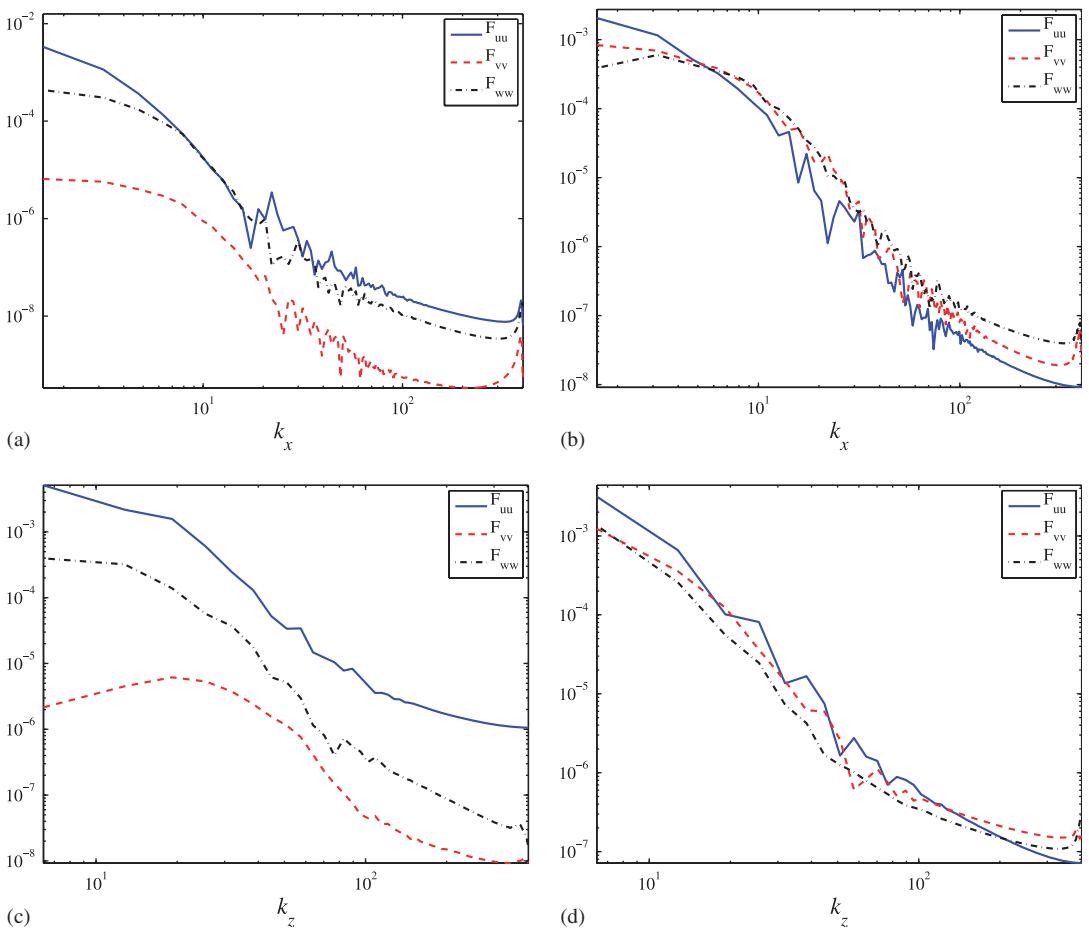

Figure 12. One-dimensional spectra: (a) $y_+ = 5.39$ (streamwise separation); (b) $y_+ = 149.23$ (streamwise separation); (c) $y_+ = 5.39$ (spanwise separation); and (d) $y_+ = 149.23$ (spanwise separation).

velocity field on the new grid. Assuming that the simulation needs to simulate a certain Re_τ with a given number of grid points in the wall-normal direction, which leads to channel half height of H, then the viscosity of the new simulation can be modified to

$$\nu = \frac{\mathrm{d}U/\mathrm{d}y}{(Re_\tau/H)^2} \tag{36}$$

which would also define an expected friction velocity of

$$u_\tau = \sqrt{\nu \frac{\mathrm{d}U}{\mathrm{d}y}} \tag{37}$$

DOI: 10.1002/fld

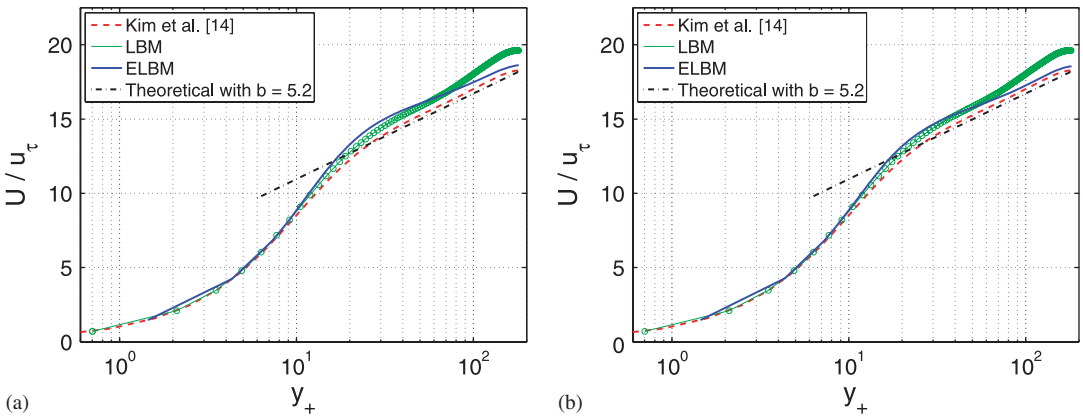

Figure 13. Comparison of ELBM and traditional pseudo-spectral methods for mean velocity profiles. Averages are taken in time and space over the last 107.5 thousand time steps. Based on the input parameters the theoretical value of Re_τ is 180: (a) upper wall ($Re_\tau = 185$) and (b) lower wall ($Re_\tau = 186$).

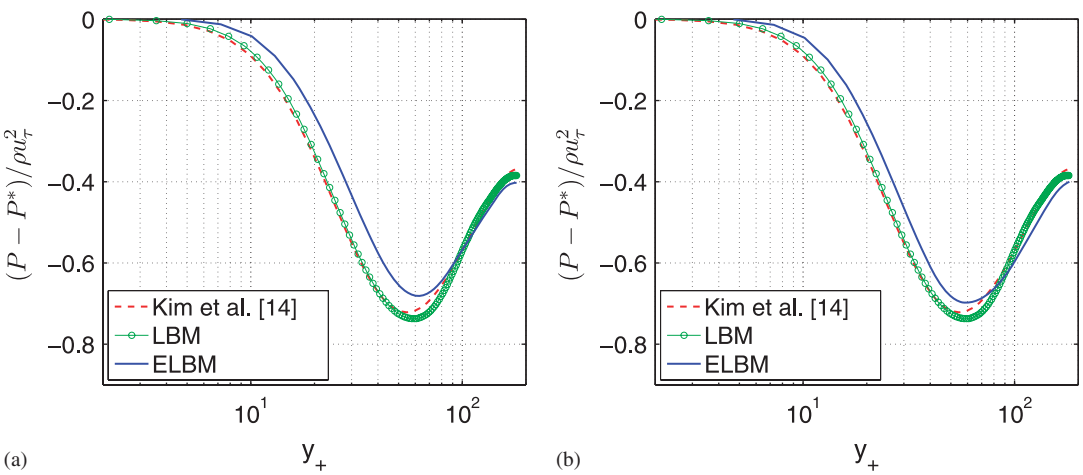

Figure 14. Comparison of ELBM and traditional pseudo-spectral methods for mean pressure profiles. Averages are taken in time and space over the last 107.5 thousand time steps: (a) upper wall ($Re_\tau = 185$) and (b) lower wall ($Re_\tau = 186$).

The pressure gradient can then be found through

$$G = \frac{u_\tau^2 \rho}{H} \tag{38}$$

This gives all the needed input parameters for the new simulation.

The ELBM simulation was based on Equation (12). The number of grid points was reduced by a factor of two in the wall-normal direction only (128 points from plate to plate). The form of the equilibrium function and the method used for solving the entropy condition were taken from [7].

DOI: 10.1002/fld

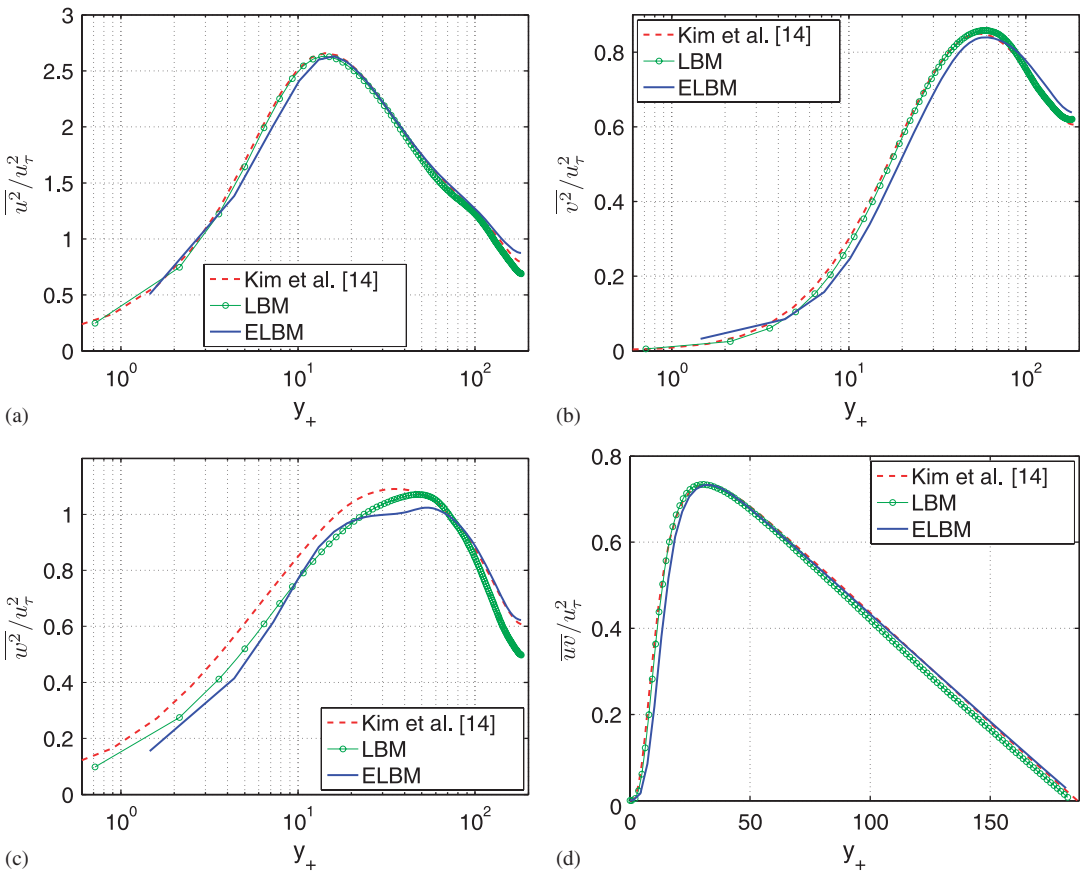

Figure 15. Comparison of ELBM and traditional pseudo-spectral methods for Reynolds stresses at the lower wall. Averages are taken in time and space over 4.3×10^5 time steps.

With this grid resolution the regular LBGK (1) becomes unstable. Similar to the previous section, the mean velocity and pressure fields from the ELBM low-resolution simulation are recorded and compared with the pseudo-spectral DNS of Kim *et al.* [14]. All of them (Figures 13–16) show very good agreement both with pseudo-spectral DNS and with LBM DNS. The only problem seems to be the r.m.s value of the pressure fluctuations. It must be noted here that one cannot go to very low grid resolution and still obtain accurate results. For example, when the grid was reduced by a factor of 4 (64 grid points from plate to plate) the simulation produced results, which were inaccurate in an obvious way—the velocity profile contained many discontinuities.

3. CONCLUSIONS

We have completed a turbulent channel flow simulation using the LBM. We used both the regular LBM with a grid resolution that was fine enough to resolve the smallest flow structures, resulting

DOI: 10.1002/fld

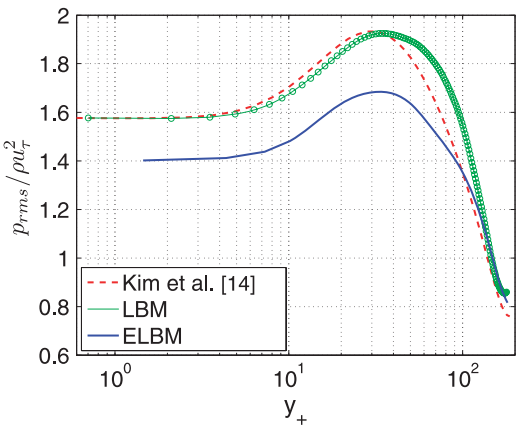

Figure 16. Comparison of ELBM and traditional pseudo-spectral methods for the r.m.s. values of the pressure fluctuations at the lower wall. Averages are taken in time and space over 4.3×10^5 time steps.

in a DNS-type computation, and the ELBM was used to redo the same simulation with a reduced number of grid points. Results from both of these simulations showed excellent agreement with the already existing data. Keeping in mind that Lammers *et al.* [8] have shown that LBM is more efficient on parallel computers than regular numerical schemes, and that additional physics are easily implemented within the method, certain problems that are not straightforward to solve with regular numerical techniques and with today's computers might be successfully tackled with LBM (e.g. turbulent multiphase flow in complex geometries). However, there are some problems that might appear. Most of them come from the fact that LBM is a novel method and some techniques one is used to having available with regular numerical techniques might either be absent or not well developed within the LBM framework.

An example of such a problematic issue for the current study was the no-slip boundary condition. Different schemes were attempted. Eventually, the halfway bounce-back method gave the best results with this particular geometry and Reynolds number regime. The authors' implementation of other schemes introduced instabilities or large errors into the simulations. The halfway bounce-back scheme is simple but it could also introduce instabilities (to a smaller extent but the problem exists) and works only if the boundary is aligned with the grid.

During the course of the current study an idea was born for a different way to implement non-decreasing entropy. The current ELBM solves for α, which is related to the maximum relaxation point toward local equilibrium for every grid point inside the domain. The solution value is usually different from $\alpha = 2$, which is the value required to preserve the viscosity during the collision step. Then the relaxation parameter is multiplied by the new value. This means that the viscosity (inversely related to the relaxation parameter) in the domain is changed at every grid point at each time step, regardless of the grid point actually satisfying the entropy requirement or not. An alternative approach to this could be to check first if the collision is going to decrease the entropy and only in this case to calculate α and subsequently modify the viscosity appropriately. This would lead to less computations per time step and avoid unnecessary modifications of the viscosity. The current ELBM works because it probably changes the viscosity slightly, not only decreasing it, but also increasing it sporadically.

DOI: 10.1002/fld

Based on the results from our numerical experiments and the theory behind LBM it can be concluded that it is a promising tool for simulations of high-Re flows. DNS of flows in complex geometries on parallel computers can be executed with ease. If the desired grid resolution cannot be achieved then ELBM can be used to stabilize the simulation and produce accurate results.

ACKNOWLEDGEMENTS

This work was supported by ONR grant number N000140510914.

REFERENCES

1. Succi S. *The Lattice Boltzmann Equation for Fluid Dynamics and Beyond*. Oxford University Press: Oxford, 2001.
2. Chen S, Doolen G. Lattice Boltzmann method for fluid flows. *Annual Review of Fluid Mechanics* 1998; **30**:329–364.
3. Qian YH, D'Humières D, Lallemand P. Lattice BGK models for Navier–Stokes equation. *Europhysics Letters* 1992; **17**(6):479–484.
4. Keating B, Vahala G, Yepez J, Soe M, Vahala L. Entropic Lattice Boltzmann representations required to recover Navier–Stokes flows. *Physical Review E* (*Statistical*, *Nonlinear*, *and Soft Matter Physics*) 2007; **75**(3):036712–036723.
5. Chopard B, Droz M. *Cellular Automata Modeling of Physical Systems*. Cambridge University Press: Cambridge, 1998.
6. Frisch U, d'Humieres D, Hasslacher B, Lallemand P, Pomeau Y, Rivet JP. Lattice gas hydrodynamics in two and three dimensions. *Complex Systems* 1987; **1**:649–707.
7. Chikatamarla S, Ansumali S, Karlin IV. Entropic Lattice Boltzmann models for hydrodynamics in three dimensions. *Physical Review Letters* 2006; **97**(1):010201.
8. Lammers P, Beronov KN, Volkert R, Brenner G, Durst F. Lattice BGK direct numerical simulation of fully developed turbulence in incompressible plane channel flow. *Computers and Fluids* 2006; **35**(10):1137–1153.
9. Tennekes H, Lumley J. *A First Course in Turbulence*. MIT Press: Cambridge, MA, 1972.
10. Amati G, Succi S, Piva R. Massively parallel Lattice–Boltzmann simulation of turbulent channel flow. *International Journal of Modern Physics C* 1997; **8**:869–877.
11. Jimenez J, Moin P. The minimal flow unit in near-wall turbulence. *Journal of Fluid Mechanics* 1991; **225**:213–240.
12. Hou S, Zou Q. Simulation of cavity flow by the Lattice Boltzmann method. *Journal of Computational Physics* 1995; **118**:329–347.
13. He X, Zuo Q, Luo L, Dembo M. Analytic solutions of simple flows and analysis of nonslip boundary conditions for the Lattice Boltzmann BGK model. *Journal of Statistical Physics* 1997; **87**(1–2):115–136.
14. Kim J, Moin P, Moser R. Turbulence statistics in fully developed channel flow at low Reynolds number. *Journal of Fluid Mechanics* 1987; **177**:133–166.

DOI: 10.1002/fld